

On Dyson-Schwinger equations and the number of fermion families

Davor Palle

Zavod za teorijsku fiziku, Institut Rugjer Bošković

Bijenička cesta 54, 10001 Zagreb, Croatia

(Dated: November 25, 2009)

Abstract

We study Dyson-Schwinger equations for propagators of Dirac fermions interacting with a massive gauge boson in the ladder approximation. The equations have the form of the coupled nonlinear integral Fredholm equations of the second kind in the spacelike domain. The solutions in the time-like domain are completely defined by evaluations of integrals of the spacelike domain solutions. We solve the equations and analyze the behavior of solutions on the mass of the gauge boson, the coupling constant, and the ultraviolet cutoff. We find that there are at least two solutions for the fixed gauge boson mass, coupling, and the ultraviolet cutoff, thus there are at least two fermion families. The zero-node solution represents the heaviest Dirac fermion state, while the one-node solution is the lighter one. The mass gap between the two families is of the order of magnitude observed in nature.

PACS numbers: 11.15.-q; 11.15.Ex

arXiv:hep-ph/0703203v3 25 Nov 2009

I. INTRODUCTION AND MOTIVATION

There is a common belief in particle physics that the Higgs mechanism resolves the problem of generating the masses of particles, although the masses of gauge bosons and fermions are fixed by couplings to Higgs scalars that are completely free parameters. The observed pattern of fermion and gauge boson masses should stimulate a search for a better symmetry breaking mechanism. The example of such a symmetry breaking mechanism is the proposed principle of noncontractible space [1].

It is assumed that the origin of the broken conformal, discrete, and gauge symmetries in particle physics is hidden in the character of the physical space, namely its noncontractibility. The appearance of the chirally asymmetric coupling of SU(2) gauge bosons to leptons and quarks, the appearance of the massive SU(2) gauge bosons and very heavy and very light Majorana neutrinos, the relation between fermion and gauge boson mixing angles, etc., are just consequences of mathematical consistency requirements of the proposed SU(3) conformal unification scheme of strong and electroweak forces. The universal ultraviolet cutoff (minimal universal scale or distance) is fixed by the mass of weak gauge bosons [1, 2]

$$\Lambda = \frac{2\pi}{\sqrt{6}g_w}M_W, \quad g_w = e/\sin \Theta_W, \quad \alpha_e = \frac{e^2}{4\pi} \implies \Lambda = 321.3\text{GeV}. \quad (1)$$

It was shown that heavy Majorana neutrinos could be perfect candidate particles for cold dark matter [3] because they are cosmologically stable owing to the absence of Higgs scalars in the theory. They are probably already indirectly observed in the center of our galaxy by atmospheric Čerenkov telescopes [4]. The universality of the minimal scale is confirmed by the Einstein-Cartan quantum theory of gravity that can resolve cosmological problems without inflaton scalar fields [5]. The prediction of the Einstein-Cartan cosmology for the negative cosmological constant (or the negative contribution of torsion and zero cosmological constant) can explain the low power of the large-angle CMBR data by the integrated Sachs-Wolfe effect if the Hubble constant is small (or large). If the total angular momentum of the Universe is large at present then the Hubble constant could be also large explaining the anomalous large scale flows of the Universe [6]. The rotating Universe is a natural consequence of the Einstein-Cartan cosmology with spinning hot and cold dark matter particles [7]. This vorticity can be studied by CMBR (WMAP)[8] or by SDSS data [9].

Having not only renormalizable theory [10], but also ultraviolet finite gauge theory to describe the world of particle physics, one is faced with a possibility to resolve the complete structure of all Green functions of the theory studying the respective Dyson-Schwinger equations. We start this difficult task in the present paper by the study of Dyson-Schwinger equations for Dirac fermion propagators in the ladder approximation where fermions are coupled to one massive gauge boson. We give the respective equations and necessary algorithms to solve these equations in the next section, while the results and thorough analyses and discussion are given in the last section.

II. EQUATIONS AND ALGORITHMS

We assume that Dirac fermions couple chirally symmetric to one massive gauge boson by the standard form ($M \equiv$ gauge boson mass), thus we study the Abelian chirally symmetric version of the BY theory of the Ref.[1]:

$$\begin{aligned} \mathcal{L} &= \bar{\Psi}_D (\not{\partial} - g \not{A}) \Psi_D - \frac{1}{4} F_{\mu\nu} F^{\mu\nu} + \mathcal{L}_{g.f.} \\ &\quad + (\partial_\mu \Phi^* + ig A_\mu \Phi^*) (\partial^\mu \Phi - ig A^\mu \Phi) - (Y_M \bar{\Psi}_D \Phi^* \Psi_D^c + h.c.), \end{aligned} \quad (2)$$

$\mathcal{L}_{g.f.} =$ standard gauge fixing terms, $\Psi_D^c \equiv$ charge conjugated Ψ_D ,

$$F_{\mu\nu} = \partial_\mu A_\nu - \partial_\nu A_\mu, \quad \Phi = v + i\chi, \quad M = \sqrt{2}gv.$$

The renormalizability and gauge invariance are ensured by the coupling of the Nambu-Goldstone boson to the gauge boson and the Majorana fermion as in [1]. We assume also that Nambu-Goldstone bosons carry lepton number as in the BY theory of Ref.[1], thus only Majorana bare mass term is allowed. The symmetry breaking parameter v is in this model free parameter and it is not fixed by the Wick's theorem as in the non-Abelian version BY of [1]. We study only equations of a Dirac fermion in this paper.

The Dirac fermion propagator is defined as $S'_F(p) = [\alpha(p) \not{p} - \beta(p)]^{-1}$. It is advantageous to write Dyson-Schwinger equations for fermion propagators in the ladder approximation [11], in the Landau gauge. Then, the equations have the following form in the spacelike domain:

$$\begin{aligned}
\beta(x) &= C \int_0^{\Lambda^2} dy K(x, y) \frac{y\beta(y)}{y\alpha^2(y) + \beta^2(y)}, \\
\alpha(x) &= 1 - C \int_0^{\Lambda^2} dy L(x, y) \frac{y\alpha(y)}{y\alpha^2(y) + \beta^2(y)}, \\
x &\equiv p^2, \quad C \equiv \alpha_g/\pi \equiv \frac{g^2}{4\pi^2}, \quad K(x, y) = \frac{3}{2} \left(1 + \frac{M^2}{3s}\right) \frac{1}{x + y + M^2 + s}, \\
L(x, y) &= \frac{yM^2}{s(x + y + M^2 + s)^2}, \quad s = [(x + y + M^2)^2 - 4xy]^{1/2}.
\end{aligned} \tag{3}$$

One has to add one more term in the timelike domain because of the existence of the branch point of kernels and a correct analytical continuation [10, 11]:

$$\begin{aligned}
\beta(x) &= C \int_0^{\Lambda^2} dy K(x, y) \frac{y\beta(y)}{y\alpha^2(y) + \beta^2(y)} \\
&\quad + \Theta(\sqrt{-x} - M) C \int_{-(\sqrt{-x}-M)^2}^0 dy \Delta K(x, y) \frac{y\beta(y)}{y\alpha^2(y) + \beta^2(y)}, \\
\alpha(x) &= 1 - C \int_0^{\Lambda^2} dy L(x, y) \frac{y\alpha(y)}{y\alpha^2(y) + \beta^2(y)} \\
&\quad - \Theta(\sqrt{-x} - M) C \int_{-(\sqrt{-x}-M)^2}^0 dy \Delta L(x, y) \frac{y\alpha(y)}{y\alpha^2(y) + \beta^2(y)},
\end{aligned} \tag{4}$$

$$s = it, \quad t^2 = 4xy - (x + y + M^2)^2, \quad \Delta K \equiv K(x, y, s) - K(x, y, s^*),$$

$$\begin{aligned}
\Delta L &\equiv L(x, y, s) - L(x, y, s^*) \\
\Rightarrow \Delta K(x, y) &= -\frac{3s}{4xy} + \frac{M^2(x + y + M^2)}{4xys}, \\
\Delta L(x, y) &= \frac{M^2}{4yx^2s} [(x + y + M^2)^2 - 2xy].
\end{aligned}$$

Now we shall describe in detail how we solve equations, while analyses of solutions are left for the final section.

We solve equations in four steps.

Step 1:

The equations in the spacelike domain have the form of the coupled nonlinear Fredholm integral equations of the second kind [12] and we need the initial guess functions to proceed further. A good choice is a solution of the nonlinear equations for the vanishing gauge boson mass. In this case, the nonlinear integral equations are reduced to nonlinear differential equations [11]:

$$(4x \frac{d^2}{dx^2} + 8 \frac{d}{dx})B(x) = -3C \frac{B(x)}{x + B^2(x)}, \quad \beta = B, \quad \alpha = 1. \quad (5)$$

This equation is solved by the Adams-Bashforth method. One can easily find initial conditions from the equation and using the rule of de l'Hôpital at $x = p^2 = 0$:

$$\frac{dB}{dx}(0) = -\frac{3}{8} \frac{C}{B(0)}, \quad \frac{d^2B}{dx^2}(0) = -\frac{3C^2}{32B^3(0)}.$$

The asymptotic of the solution at large spacelike momenta gives us a condition to find the solution with an arbitrary number of nodes

$$\frac{dB}{dx}(x = \Lambda_i^2) + \frac{B(x = \Lambda_i^2)}{\Lambda_i^2} = 0.$$

One can simply generate solutions from fixed initial conditions at the zero momentum and then search for momenta which fulfill above condition. As an example, for $C = 0.7$ and $B(0) = 1GeV$, one obtains j -node solutions with the following Λ_j cutoffs: $\Lambda_0 = 4.292GeV$, $\Lambda_1 = 85.82GeV$ and $\Lambda_2 = 1715.87GeV$.

Thus we can generate initial guess functions by $\beta = B$ and $\alpha = 1$. Assuming the existence of the fundamental cutoff Λ , one has to rescale all dimensional quantities of a certain dimension k by multiplication with $(\Lambda/\Lambda_i)^k$ at the end of the calculation with the cutoff Λ_i .

Step 2:

Using the initial guess functions, we have to choose the method how to solve nonlinear integral equations. Between Nyström, Galerkin or the collocation method [12], or Newton-like iterations [13], we decide to implement the collocation method.

It is more comfortable to work with logarithmic variables in the spacelike domain, thus we change the variables to $w = \ln(1 + x/B(0)^2)$. The β and α functions are approximated by Čebišev polynomials:

$$f(x) \approx -\frac{1}{2}c_1 + \sum_{k=1}^N c_k T_{k-1}(x), \quad -1 \leq x \leq +1.$$

Inserting $\tilde{\beta}$ and $\tilde{\alpha}$ into the Fredholm equations, Eq.(3), we obtain a nonlinear algebraic system of equations for the set of coefficients $\{b_i, a_j\}$ in Eq. (6). This system of equations is solved by the modified Powell hybrid method [14].

We divide the integration region for a one-node solution into two segments $0 \leq x \leq \Lambda_0^2$ and $\Lambda_0^2 \leq x \leq \Lambda_1^2$, and write the approximate solutions $\tilde{\beta}$ and $\tilde{\alpha}$ with two separate Čebišev expansions, one for every segment. The accuracy of the approximation is improved, but the number of variables is twice compared with the zero-node case. Usually, we take 20 Čebišev polynomials in one approximation, thus $2 \times 2 \times 20 = 80$ coefficients as variables for one-node solution, 40 for zero-node, 160 for two-node solution, etc. We define the discretized sequence of the corresponding logarithmic variables w_i in each segment that is distributed homogeneously, except for a denser distribution of points at the joint of two segments. The corresponding number of nonlinear algebraic equations for coefficients b_i, a_j can now be formed:

$$\begin{aligned}
F_{1,i} &\equiv \tilde{\beta}(w_i) - CB(0)^2 \int_0^{w_\Lambda} dw' e^{w'} K(x(w_i), y(w')) \frac{y(w') \tilde{\beta}(w')}{y(w') \tilde{\alpha}^2(w') + \tilde{\beta}^2(w')} = 0, \\
F_{2,i} &\equiv \tilde{\alpha}(w_i) - 1 + CB(0)^2 \int_0^{w_\Lambda} dw' e^{w'} L(x(w_i), y(w')) \frac{y(w') \tilde{\alpha}(w')}{y(w') \tilde{\alpha}^2(w') + \tilde{\beta}^2(w')} = 0, \\
i &= 1, \dots, n,
\end{aligned} \tag{6}$$

$$\begin{aligned}
\tilde{\beta}(w) &= \sum_{k=1}^n b_k T_{k-1}(\bar{w}), \quad \tilde{\alpha}(w) = \sum_{k=1}^n a_k T_{k-1}(\bar{w}), \quad \bar{w} = \frac{2w}{w_\Lambda} - 1, \\
w_\Lambda &= \ln(1 + \Lambda^2/B(0)^2), \quad x(w) = B(0)^2(e^w - 1), \quad y(w) = B(0)^2(e^w - 1).
\end{aligned}$$

To this system, we apply the modified Powell hybrid method and verify the result of the computation.

Step 3:

If we obtain a solution even under small tolerance, one has to verify it with a very large number of arguments w (more than 1000) for both $\tilde{\beta}$ and $\tilde{\alpha}$ and check the errors. One can expect larger errors for higher-node solutions.

The final check whether our solution is a real solution or only some local minimum must be performed by solving the system once more, but now with a more precise approximation scheme, namely, the piecewise cubic spline method.

The variables are now values of $\tilde{\beta}$ and $\tilde{\alpha}$ functions evaluated for 200 arguments w_i and we form equations as was done previously for Čebišev coefficients. Thus, we solve an algebraic system with 400 variables using the modified Powell hybrid method. Note that for every solution (β, α) there is also a solution $(-\beta, \alpha)$. If the procedure does not diverge or does not end with a trivial solution, we have a very accurate solution in the spacelike domain that should be checked explicitly once more.

Step 4:

It is obvious that the relations in Eq.(4) are not equations for the timelike domain, but just formulas for evaluations of β and α in the timelike domain, knowing their solutions in the spacelike domain.

Namely, let us define the following intervals: $I_0 = \{x|0 \leq x \leq \Lambda^2\}$ and $I_j = I_0 \cup \{x|0 \geq x \geq -(j \times M)^2\}$. From the boundaries of integrals in Eq.(4) one can conclude that the timelike part of I_1 is defined by integration over I_0 , similarly, the timelike part of I_2 is defined by integration over I_1 , etc. The procedure can be continued to arbitrary I_k .

Note that the integrals over timelike domains are very well defined by the endpoint singularity integration. The endpoint singularity at $y = -(\sqrt{x} - M)^2$ of kernels ΔK and ΔL is integrable.

If the propagator reaches the mass singularity for a certain $x = -m_f^2 \in I_k$, then at $x = -(m_f + M)^2 \in I_{k+1}$ the functions β and α diverge because the endpoint singularity becomes nonintegrable. However, the mass function $\mu(x) \equiv \beta(x)/\alpha(x)$ is even at this point well defined as the limes of the quotient ∞/∞ . Anyhow, the numerics in the interval I_{k+1} in the vicinity of $x = -(m_f + M)^2$ is becoming difficult, so we stop our calculation at I_k .

We perform integrations using the Gauss-Kronrod and Clenshaw-Curtis methods which we have checked using the slow and accurate Monte Carlo method. The functions β and α are approximated in the timelike part of I_k by piecewise cubic spline with 800 values for each function.

This completes our procedure of solving Dyson-Schwinger equations for fermion propagators. The next section is devoted to results and physical implications.

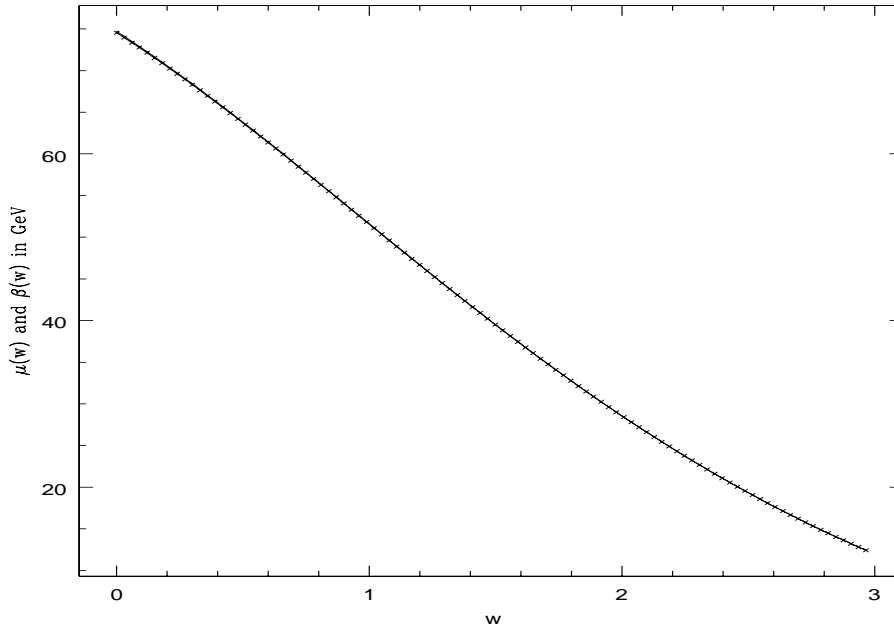


FIG. 1: This figure depicts the mass-function μ (solid line) and the β -function (crosses) in the spacelike domain for a zero-node solution and parameters $C = 0.7$, $M = 3.5\text{GeV}$, $\Lambda = 321.3\text{GeV}$. "w" is a logarithmic variable defined by $B(0) = 1\text{GeV}$.

III. RESULTS AND DISCUSSION

The results presented in this paper are only those that have passed our procedure in four steps. The fact that the procedure fails in certain cases does not mean that the equations do not necessarily have solutions. The proof of the existence of any kind of solutions is not attempted in this paper.

Our experience with these equations tells us that our procedure fails to find solutions for higher gauge boson mass, one-node solutions for coupling close to the critical $C = \frac{1}{3}$, and two- or higher-node solutions for any coupling. However, we find enough solutions to make relevant physical conclusions and suggestions for the improvement of algorithms. The attempt to find a solution by perturbing parameters, such as coupling or boson mass, is usually not successful.

The reader can visualize solutions with zero and one node in Figs.1-4, where the mass function is defined as $\mu \equiv \beta/\alpha$ and $m_f \equiv$ fermion mass.

That zero-node solutions are heavier than one-node solutions can be seen from Figs. 1-5.

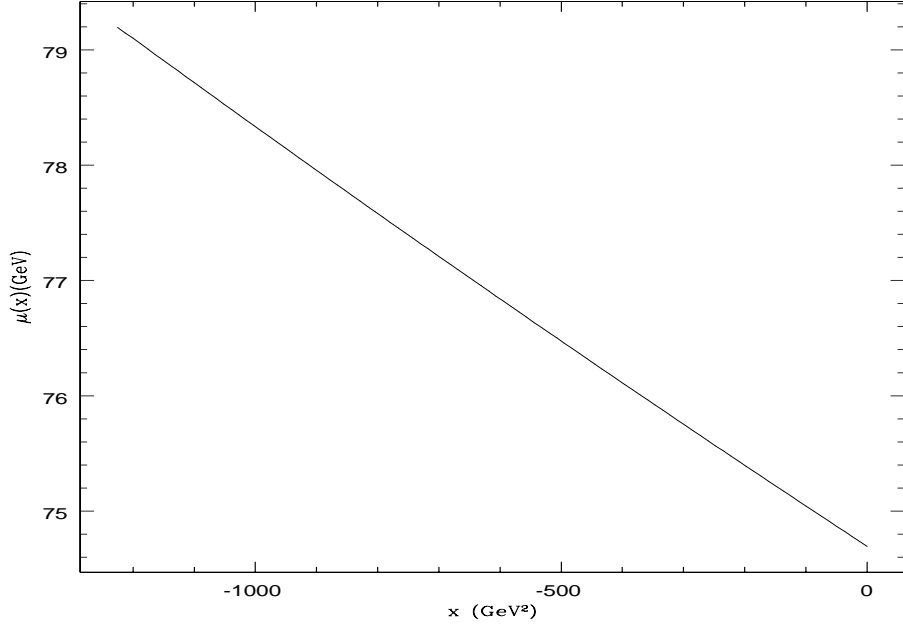


FIG. 2: This figure depicts the mass-function μ in the timelike domain for a zero-node solution and parameters $C = 0.7$, $M = 3.5\text{GeV}$, $\Lambda = 321.3\text{GeV}$.

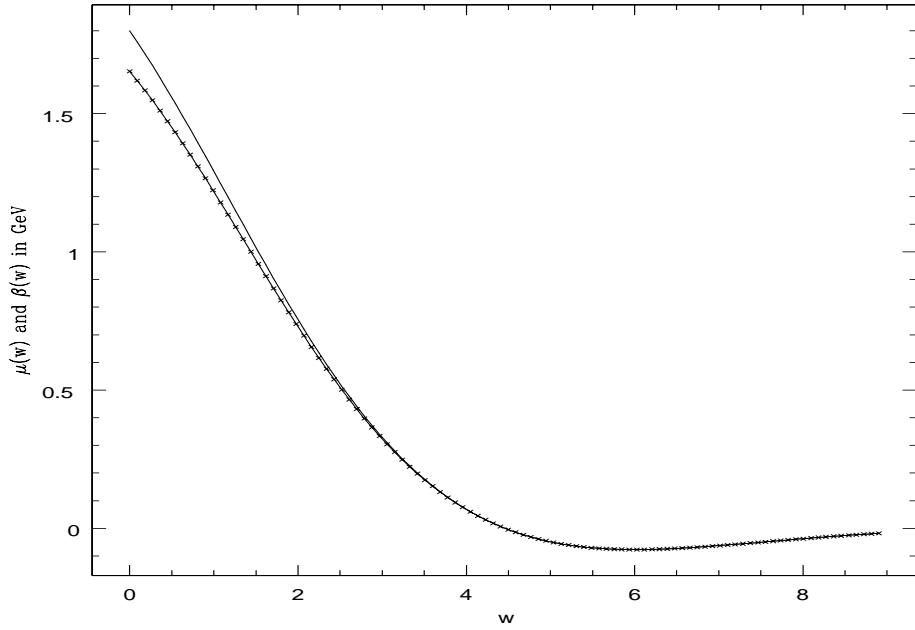


FIG. 3: The mass-function μ (solid line) and the β -function (crosses) in the spacelike domain for a one-node solution and parameters $C = 0.7$, $M = 3.5\text{GeV}$, $\Lambda = 321.3\text{GeV}$. "w" is a logarithmic variable defined by $B(0) = 1\text{GeV}$.

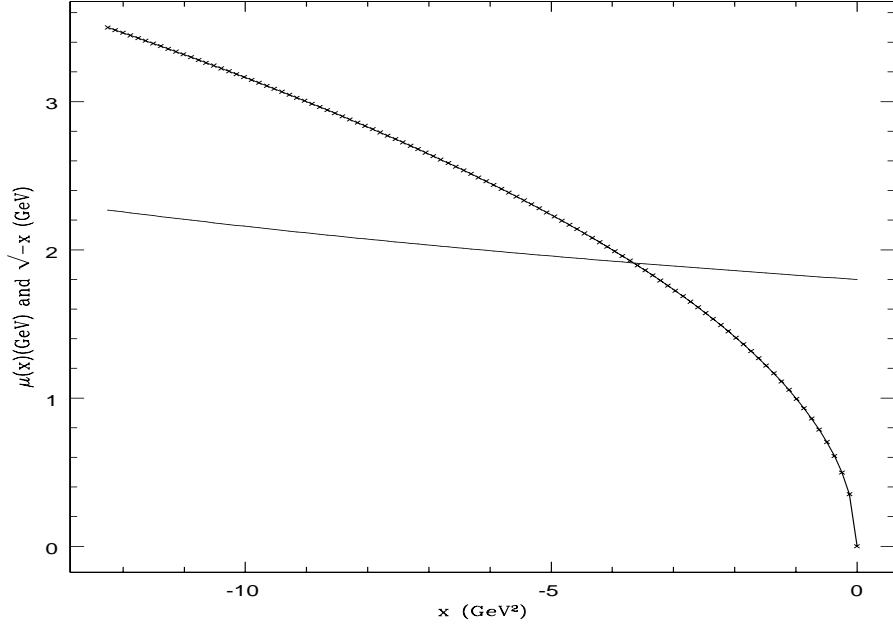


FIG. 4: The mass-function $\mu(x)$ (solid line) and $\sqrt{-x}$ (crosses) plotted in the timelike domain for a one-node solution and parameters $C = 0.7$, $M = 3.5\text{GeV}$, $\Lambda = 321.3\text{GeV}$.

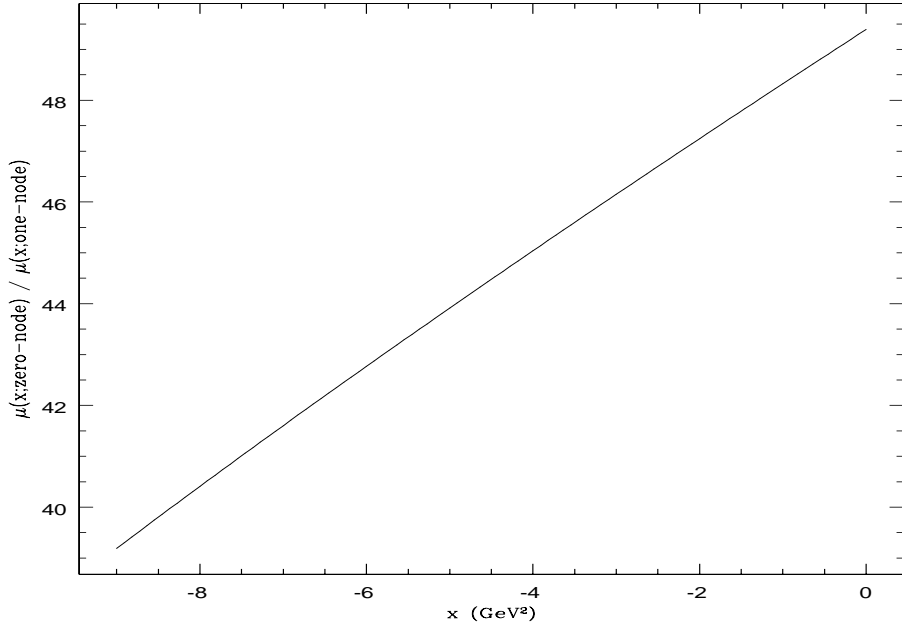


FIG. 5: The quotient of the mass-functions μ of zero-node and one-node solutions in the timelike domain for parameters $C = 0.75$, $M = 3.0\text{GeV}$, $\Lambda = 321.3\text{GeV}$.

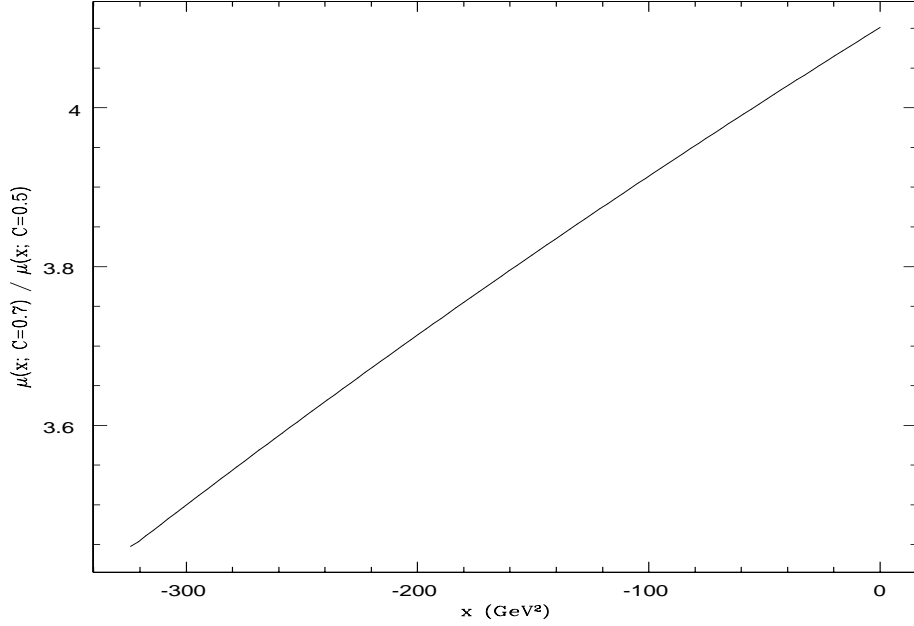


FIG. 6: The quotient of the mass-functions μ of zero-node solutions for $C = 0.7$ and $C = 0.5$ in the timelike domain and parameters $M = 4.5\text{GeV}$, $\Lambda = 321.3\text{GeV}$.

$M(\text{GeV})$	2.0	2.5	3.0	3.5	4.0	4.5
$m_f(\text{GeV})$	-	4.932	2.528	1.912	1.310	0.642

TABLE I: The dependence of m_f on the gauge boson mass M for a one-node solution with $\Lambda = 321.3\text{GeV}$ and $C = 0.7$; sign "-" denotes the absence of the mass singularity

Equations (3) have solutions only in the strong coupling regime $C \equiv \alpha_g/\pi > \frac{1}{3}$. Verifying the asymptotics of the zero-node solutions in the timelike domain, one can conclude on the absence of the mass singularity for couplings or gauge-boson masses when we have nontrivial solutions. This is a consequence of the strong coupling between fermions and the gauge boson. Usually, the one-node solutions have mass singularity (see Tables 1-3), unless one reaches a very strong coupling regime.

C	0.65	0.675	0.70	0.725	0.75
$m_f(\text{GeV})$	0.351	1.401	2.528	5.833	-

TABLE II: The dependence of m_f on the coupling constant C for a one-node solution with $\Lambda = 321.3\text{GeV}$ and $M = 3.0\text{GeV}$

$\Lambda(GeV)$	214.2	241.0	275.4	321.3	482.0
$m_f(GeV)$	0.428	0.983	1.639	2.528	-

TABLE III: The behavior of m_f on the fundamental cutoff Λ for a one-node solution with $M = 3GeV$ and $C = 0.7$

$M(GeV)$	6.0	8.0	10.0	12.0	14.0	16.0	18.0
$m_f(GeV)$	-	22.43	15.27	23.90	9.84	7.24	4.44

TABLE IV: The behavior of m_f on the gauge boson mass M for a zero-node solution with $\Lambda = 321.3GeV$ and $C = 0.5$ in the "model" case $\alpha \equiv 1$

The "model" case when $\alpha \equiv 1$ is studied for zero-node solutions with results in Table 4, where one can see the appearance of the mass singularity and its behavior on the gauge boson mass. The same "model" is studied in [15] but it is deficient because of various reasons: (1) it is not gauge invariant within a ladder approximation, (2) nontrivial solutions emerge only in the strong coupling regime, so α function affects crucially the mass function and cannot be set to 1, (3) according to the discussion in Step 4 of the description of the solving-procedure it is evident that the mass function contains spurious unphysical singularity in the segment I_{k+1} in the timelike domain if we put $\alpha \equiv 1$.

The behavior of the mass of the one-node solutions on the gauge boson mass can be read in Table 1. Fermion masses are very sensitive to the boson mass and they are larger for smaller boson masses. This is the expected feature, because the fermion mass singularity disappears for the vanishing boson mass [11].

Larger coupling implies larger fermion self-energy, thus also larger fermion masses, as one can read from Table 2. By rescaling of cutoffs and masses in Table 1, in Table 3 we show the dependence of fermion masses on the fundamental cutoff for the fixed boson mass. The guess that larger cutoff means larger self-energy and consequently larger masses is completely

C	0.65	0.65	0.70	0.70	0.75	0.75
n	0	1	0	1	0	1
b_{UV}	-1.003	-1.0015	-1.0021	-1.00937	-1.0014	-1.0076

TABLE V: The UV asymptotic index b_{UV} for various couplings C, $M=3 GeV$ and $\Lambda = 321.3GeV$; n=number of nodes.

confirmed.

Similar dependencies are valid for zero-node fermion states. We depict some comparisons of mass functions in Fig.6.

Let us define infrared (IR) and ultraviolet (UV) asymptotics of the mass function:

$$\mu(p^2) \sim (p^2)^b : b_{IR} = \lim_{x \rightarrow 0} \frac{xd\mu(x)/dx}{\mu(x)}, b_{UV} = \lim_{x \rightarrow \Lambda^2} \frac{xd\mu(x)/dx}{\mu(x)}.$$

A direct inspection of our solutions leads to the following conclusions: (1) $b_{IR} = 0$ for $M = 0$ and $M \neq 0$, (2) $b_{UV} = -1$ for $M = 0$ and there is a small deviation from -1 for $M \neq 0$ (see Table 5).

We can now make final conclusions about solutions of Dyson-Schwinger equations. We have shown that even the most simple bootstrap system studied in this paper has at least two solutions for the fixed coupling, the gauge boson mass, and the cutoff. The heaviest solution is the zero-node solution (belonging to the third fermion family in the standard particle physics classification), while the lighter one is the one-node solution (belonging to the second fermion family). The mass gap between these two solutions is of the order of magnitude observed in nature (Figs. 1-5). We need more sophisticated approximation schemes for functions to search for higher-node solutions, thus to find the first-family member fermion. The observed behavior of the mass functions on the parameters fulfills our expectations.

One should consider our work as the starting attempt to solve the family replication problem which is not soluble with the Higgs mechanism. Two basic scenarios are possible: (1) there are only three physical solutions in the spacelike domain, (2) there are more than three solutions in the spacelike domain but only three physically acceptable also within the timelike domain. Future studies will answer which scenario will prevail.

Before turning to a more complicated electroweak system, we are expecting to see the verification of the principle of noncontractibility by the LHC. The nonresonant enhancement of the QCD amplitudes at the weak scale has been reported by the TeVatron [10], especially measuring and estimating the quotient of cross sections at two center of mass energies [16, 17]. High-luminosity measurements at the LHC could determine the ultraviolet cutoff

to high accuracy.

- [1] D. Palle, *Nuovo Cimento* **A 109**, 1535 (1996)
- [2] W. M. Yao et al., *J. Phys.* **G 33**, 1 (2006)
- [3] D. Palle, *Nuovo Cimento* **B 115**, 445 (2000); D. Palle, *ibidem* **B 118**, 747 (2003)
- [4] F. Aharonian et al., *Astron. and Astrophys.* **425**, L13 (2004); J. Albert et al., *Astrophys. J* **638**, L101 (2006)
- [5] D. Palle, *Nuovo Cimento* **B 111**, 671 (1996); D. Palle, *ibidem* **B 114**, 853 (1999)
- [6] D. Palle, preprint [arXiv:0902.1852](https://arxiv.org/abs/0902.1852) (2009)
- [7] D. Palle, preprint [arXiv:0802.2060](https://arxiv.org/abs/0802.2060) (2008)
- [8] K. Land K, J. Magueijo, *Phys. Rev. Lett.* **95**, 071301 (2005)
- [9] M. J. Longo, preprint [arXiv:0812.3437](https://arxiv.org/abs/0812.3437) (2008)
- [10] D. Palle, *Hadronic J.* **24**, 87 (2001); D. Palle, *ibidem* **24**, 469 (2001)
- [11] T. Maskawa, H. Nakajima, *Prog. Theor. Phys.* **52**, 1326 (1974); T. Maskawa, H. Nakajima, *ibidem* **54**, 860 (1975); R. Fukuda, T. Kugo, *Nucl. Phys.* **B 117**, 250 (1976)
- [12] C. T. H. Baker, *The Numerical Treatment of Integral Equations*, (Clarendon Press, Oxford 1977); K. E. Atkinson, *The Numerical Solution of Integral Equations of the Second Kind*, (Cambridge University Press, Cambridge 1997)
- [13] M. A. Hernandez, M. A. Salanova, *J. Integral Equ. and Applic.* **17**, 1 (2005)
- [14] M. J. D. Powell, in *Numerical methods for Nonlinear Algebraic Equations*, ed. by P. Rabinowitz, p.87, (Gordon and Breach, London, 1970)
- [15] G. Cheng, T. K. Kuo, *J. Math. Phys.* **35**, 6270 (1994)
- [16] B. Abbott et al. *Phys. Rev. Lett.* **86** 2523 (2001); T. Affolder, et al., *ibidem* **88**, 042001 (2002)
- [17] D. Palle, preprint [arXiv:0910.3852](https://arxiv.org/abs/0910.3852) (2009)